

Stereoscopic PIV measurements behind a 3D flapping foil producing thrust

Parker, K.¹, von Ellenrieder, K. D.² and Soria, J.¹

¹Laboratory for Turbulence Research in Aerospace & Combustion (LTRAC)

Mechanical Engineering, Monash University
Clayton Campus, Victoria, 3800 AUSTRALIA

²Dept. Ocean Engineering
Florida Atlantic University
Dania Beach, FL 33004-3023, USA

Abstract

Past qualitative dye flow visualizations behind a finite-span flapping foil have led to a model of the vortex skeleton. Subsequent 2D PIV experiments have highlighted some salient features in the proposed model but the 2D measurements reveals limited information about a highly 3D flow. This study proposes to use 3C 3D SPIV to quantitatively describe the flow geometry and test the proposed model of the vortex skeleton. This information is used to investigate the mechanisms responsible for thrust production. Preliminary results from 2D 3C SPIV behind a 3D NACA0012 flapping foil with an aspect ratio of 3, at a Strouhal number of 0.35 at the plane of symmetry reveal qualitative information about the reverse Karman vortex street. The structure as seen in the single measured plane, is phase locked with the forced flapping motion of the foil, in agreement with previous flow visualisations.

Keywords: *Strouhal number, stereoscopic particle image velocimetry, flapping/oscillating airfoil, vortical structures, unsteady aerodynamics*

Introduction

An understanding of the fluid dynamic interactions that exist in the flow behind 3D flapping foils is paramount to harnessing the potential technology that is available in the field of unsteady propulsion. Vorticity control plays an important role in manipulating the evolution of large scale structures in the flow, thereby controlling the transport of momentum in the flow. An understanding of the mechanisms responsible for vortex interactions behind heaving and pitching foils is important from a control as well as thrust-production perspective [3].

In this study a deeper understanding of any momentum transport mechanisms, that result from modification to the vortical structure behind a flapping foil, is sought. Much of our present understanding in this field comes from past research using airfoils of infinite-span (2D airfoils). Parameters have been identified for optimal thrust production using flapping foils, with up to 80% recorded [1]. The dimensionless Strouhal number has been identified as a suitable parameter to describe the thrust producing ability of a flapping foil. In a Strouhal regime of $0.25 \leq St \leq 0.35$ 2D airfoils produce thrust with maximum efficiency. The flow behind a thrust producing foil is described by a 'reverse' Karman vortex street in which the mean velocity profile resembles a jet and momentum is added to the flow. In reality, wings are three dimensional and have finite spans. In this case the wingtip vortices add another dimension of complication to the vortical interactions and structure of the flow. Cheng and Murillo [2] first raised concerns that results from studies on 2D airfoils were over-estimated. Figure 1a shows a typical qualitative flow visualizations as observed from the wingtip of the airfoil. In contrast, the presence of wingtip vortices signif-

icantly alter the typical 2D vortex sheet as shown in the flow visualisations of von Ellenrieder *et al* in figure 2. In both cases the $St = 0.35$. The flow visualizations in figure 2 suggest that the vorticity shed from the leading edge, trailing edge and wingtips are connected. Based on these flow visualisation experiments the authors propose a model of the vortical skeleton for a 3D thrust producing foil [7] shown in figure 1b.

Since dye is a passive scalar and flow visualizations are restrictive in the information that they provide, more quantitative experiments will be carried out. The purpose of this paper is to report on SPIV measurements that provide 3C 2D information of the flow for comparison with the previous flow visualisations. Of interest is the relationship between the phase averaged structure of the flow, represented by the model of the vortex skeleton in figure 1b and the forcing introduced into the flow.

Experimental Technique

Apparatus & method

The experiments are conducted in a water tunnel at the Laboratory for Turbulence Research for Aerospace & Combustion. The working section measures $500\text{mm} \times 500\text{mm} \times 1000\text{mm}$. The turbulence intensity levels in the core region is less than 0.35%. A full description of the experimental rig is provided in [4].

A NACA0012 airfoil with chord, $c = 25\text{mm}$ and $AR = 8$ is suspended vertically above the test section. The airfoil performs angular (pitch) and lateral (heave) oscillations using stepper motors. The airfoil heaves in the y direction and simultaneously pitches about the quarter-chord position. The heave-stepper motor performs the oscillations by virtue of a scotch yoke. The scotch yoke wheel can be adjusted to accommodate different heave oscillation amplitudes. The scotch yoke moves a platform on which the pitch motor is mounted. The pitch motor drives the airfoil directly. A motion control program was created in such a manner to allow different motion parameters (such as frequency, f , maximum pitch oscillation amplitude, θ_0 and phase angle between heaving and pitching oscillations, ψ) to be independently varied. Thereby allowing for various motion profiles. Potentiometers are mounted along the heave and pitch axes. These provide accurate feedback of the output trajectory of the foils. Optical triggers have been placed at various locations along the airfoil trajectory to provide the trigger signals to the laser and cameras.

The entire oscillating mechanism is mounted on a railing system above the water tunnel, allowing the airfoil setup to be moved to different locations, while the cameras and laser arrangement is kept fixed. Further details of the motion parameters of the experiment is provided in [4].

Data Acquisition

In order to quantitatively analyze the flow, digital particle image velocimetry is utilized. PIV measurements are conducted in the near wake region of the foil. A region $3.5c$ (y-direction) by $3c$ (x-direction) is captured at a magnification of 0.095. Flow visualizations by von Ellenrieder *et al* [7] suggest this to be adequate to capture the large scale structures in the flow over 1 complete forced oscillation cycle of the foil.

Two Pixelfly CCD cameras, with array sizes of $1280px \times 1024px$ each, are mounted vertically onto a 3-axis translation stage, below the test section. An angular-displacement stereo-configuration is utilized with the cameras at 65° to each other. The cameras are fitted with $55mm$ Micro Nikkor Nikon lenses at $f\#2.8$. To satisfy the Scheimpflug condition each camera axis is tilted by 3° . $11\mu m$ seed particles are illuminated by laser light from a dual-cavity New Wave Nd:Yag laser, pulsing $532nm$ light at $32mJ$. A $3mm$ thick horizontal light sheet is created in the midspan region of the airfoil using the necessary collimating optics. The SPIV setup is optimised for good image quality. A beam collector is placed on the far side wall of the test section to collect light from the laser.

Stereo Acquisition

An in-situ calibration technique is utilized similar to [5]. Calibration images are acquired for the right and left camera at several planes across the thickness of the laser sheet. Using a template-matching digital image correlation approach, the exact positions of calibration markers are found. A polynomial with cubic dependence on the in-plane components, x and y and quadratic dependence on the out-of plane component, z is used to map the displacement in the object plane to an image plane displacement. This is adequate to remove any higher order distortions one expects to encounter [5]. A least squares approach is used to determine the mapping function for the cameras and also to calculate the final displacements of the flow field.

Double exposed images are acquired in a horizontal plane bisecting the span of the wing. The laser firing is synchronized with the motion of the foil. A trigger signal from a stepper motor is sent via a breakout box, to a RT Linux control computer that regulates a return signal to activate the laser firing and the camera acquisitions. This setup is shown in figure 1c. Phase-averaged measurements are made at 8 locations within 1 heave cycle. The period of 1 heave cycle is $640ms$. 500 instantaneous images are acquired to achieve a statistical confidence of 99%, that the error in the mean is 1%. The acquired image pairs are analyzed using a multigrad cross-correlation algorithm from Soria [6]. From the stereo images, the three components of velocity u , v and w are calculated in each plane and the vorticity is derived from the velocity gradients.

Discussion of Results

The results of the stereo-PIV experiments are presented for $Re = 637$, $\psi = 90^\circ$, $\theta_0 = 5^\circ$ and $St = 0.35$. Phase averaged measurements are taken at 8 locations shown in figure 1d. The data for every 2nd phase location is presented here, representing the motion reciprocating motion of the foil in 1 cycle. The visualisations in figure 2 are at the same phase locations in order to compare to the SPIV measurements. The preliminary measurements are made in a plane bisecting the midspan of the foil where the flow exhibits greatest complexity.

From the integrated streamline patterns of figure we observe many critical points including nodes, saddle points and foci in the in-plane field. Here the convection velocity has been removed from the flow field. The orientation and location of the

airfoil in the flapping trajectory has been indicated by the inclusion of the airfoil in the right of each image. As in the case of the flow visualisation images, flow is from right to left. These results compare favourable with previous 2D PIV measurements [4]. The location and orientation of the airfoil in the flow field gives a sense of the disturbance introduced by the forcing motion of the foil. Figure shows iso-contours of the out of plane vorticity. Regions of intense vorticity. Vorticity of opposite sign is shed into the flow in 1 cycle. The vortex formations produces a reverse Karman vortex street of counter-rotating vortex pairs. From this measurement in the symmetry plane the results support the argument of phase locked vorticity control from von Ellenrieder *et al*[7]. The flow is characterized by a sequence of coherent structures of positive and negative vorticity which shed and evolve in relation to the phase of the foil. Vorticity of opposite rotation is shed at the extreme heave and pitch positions of the airfoil.

SUMMARY

The flow measured at the midspan of the foil is inherently complex and three dimensional. The flow sequence from the PIV measurements differ from the flow visualizations images. These differences are ascribed firstly, to the general limitation of flow visualizations, as passive scalar measurements. Secondly, with the current single-plane information further elaboration of the mechanisms responsible for momentum transport or vorticity evolution is speculative at best. Consequently, 3C 3D measurements are planned for the future.

ACKNOWLEDGEMENTS

The authors would like to acknowledge the support of Dr. Phillipa O'Neil and Dr. Simon Clarke in the formulation of the stereo reconstruction algorithm. Also Mr. Ivor Mackay, Mr. Eric Wirth and Mr. Adam Castle for the fabrication of the SPIV experimental rig

References

- [1] J. M. Anderson, K. Streitlien, D. S. Barrett, and M. S. Triantafyllou. Oscillating foils of high propulsive efficiency. *J. Fluid Mech.*, 360:41–72, 1998.
- [2] H.K Cheng and L. E Murillo. Lunate-tail swimming propulsion of a curved lifting line in unsteady flow. *J. Fluid Mech.*, 143:327–350, 1984.
- [3] R. Gopalkrishnan, M. S. Triantafyllou, G. S. Triantafyllou, and D. Barrett. Active vorticity control in a shear layer using a flapping foil. *J. Fluid Mech.*, 274:1–21, 1994.
- [4] Soria J. Parker K., von Ellenrieder K. D. A description of the vortical skeleton behind a finite-span flapping wing. In *Twelfth International Symposium on Applications of Laser Techniques to Fluid Mechanics*, Lisbon, Portugal, 2004.
- [5] Liu Z. C. Soloff S. M., Adrian R. J. Distortion compensation for generalized stereoscopic particle image velocimetry. *Meas. Sci. Technol.*, 8:1441–1454, 1997.
- [6] J. Soria. Multigrad approach to cross-correlation digital PIV and HPIV analysis. In *Proceedings of 13th Australasian Fluid Mechanics Conference*. Monash University, 1998.
- [7] Soria J. von Ellenrieder K. D., Parker K. Flow structures behind a heaving and pitching finite-span wing. *J. Fluid Mech.*, 490:129–138, 2003.

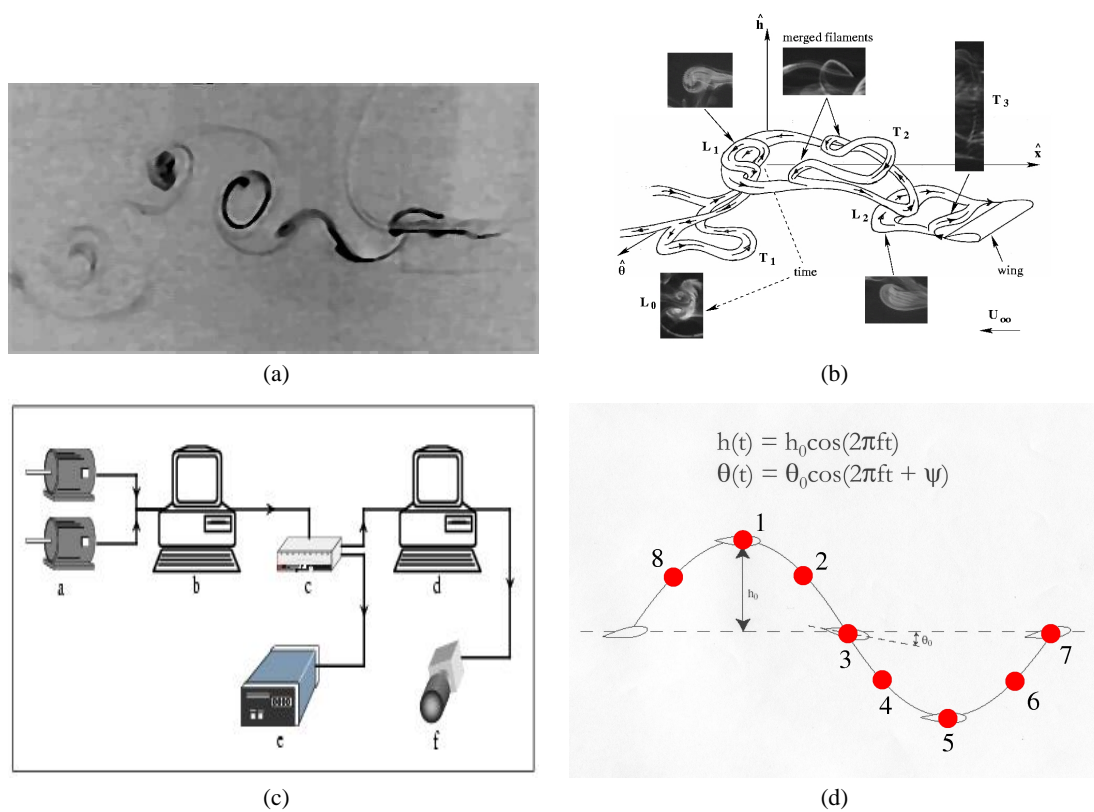


Figure 1: (a) Dye flow visualization of the flow behind a 2D flapping airfoil, (b) Proposed 3D structure of the vortex skeleton behind a 3D flapping wing. For the condition shown, $St = 0.35$, $\theta_0 = 10^\circ$ and $\psi = 90^\circ$, (c) Schematic of the data acquisition and PIV control system- a) heave and pitch motor trigger signal, b) RTLinux control PC, c) breakout box, d) camera control PC, e) CCD camera, f) Nd:Yag laser, (d) Motion profile of the flapping foil highlighting the location of the phase averaged measurements.

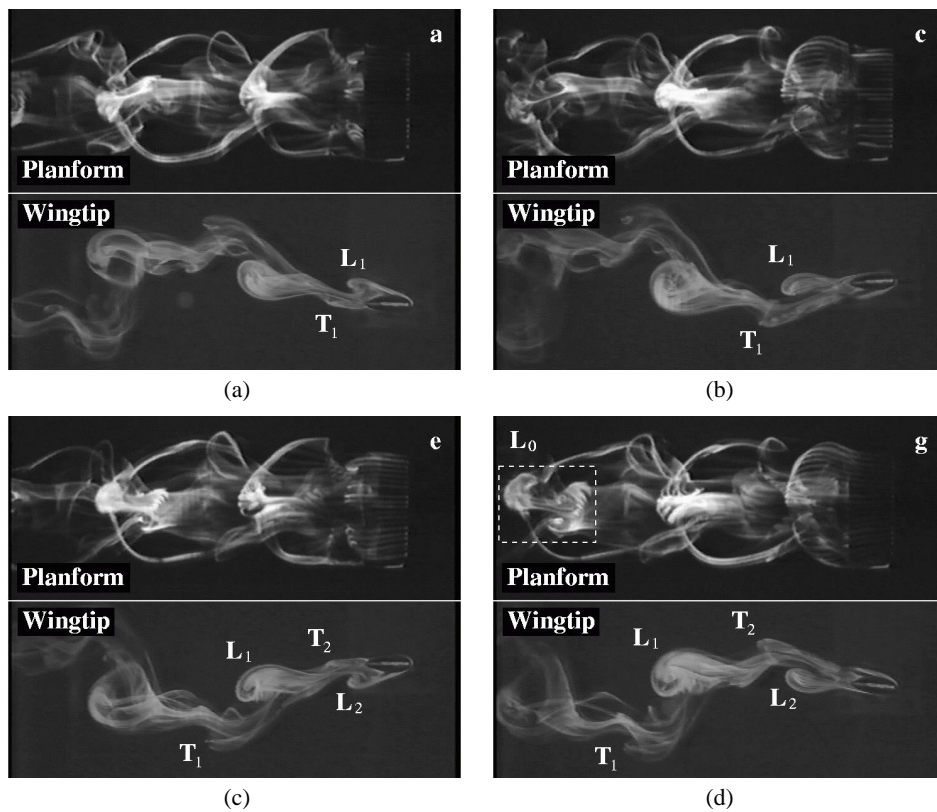


Figure 2: Dye flow visualisation of the flow behind a 3D flapping foil at $St = 0.35$. instantaneous images at: (a) phase 1, (b) phase 3, (c) phase 5, (d) phase 7.

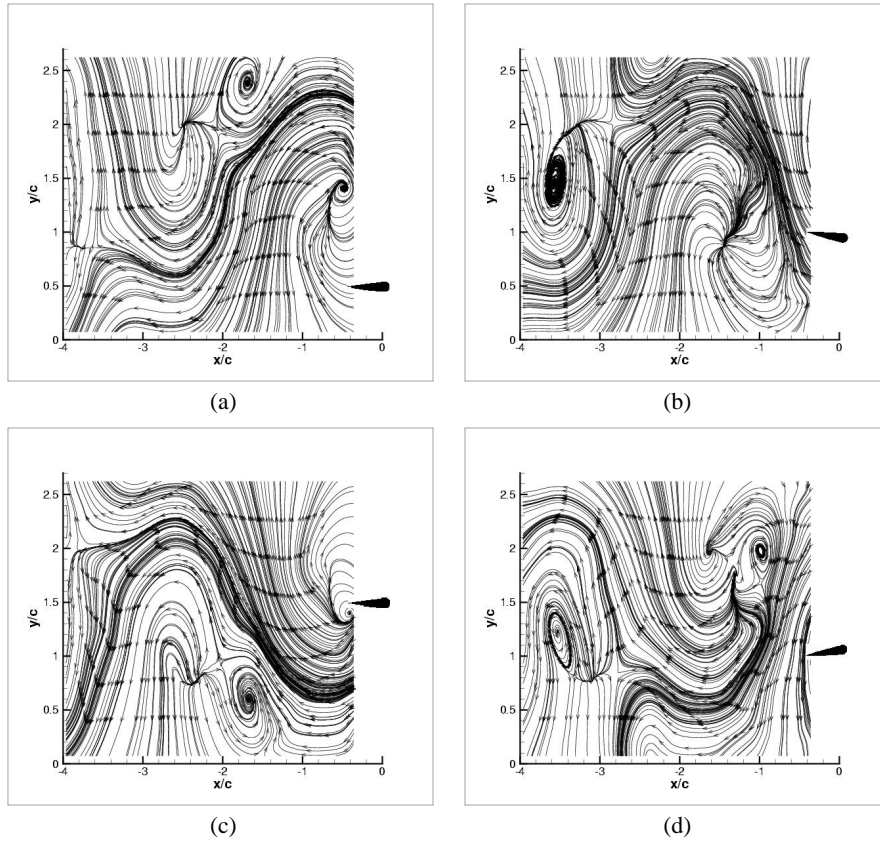


Figure 3: Integrated streamline pattern for the u, v in-plane velocity components measured behind a 3D flapping foil at (a) phase 1, (b) phase 3, (c) phase 5, (d) phase 7. In both cases the velocity components are non-dimensionalised by the freestream velocity, u_∞ .

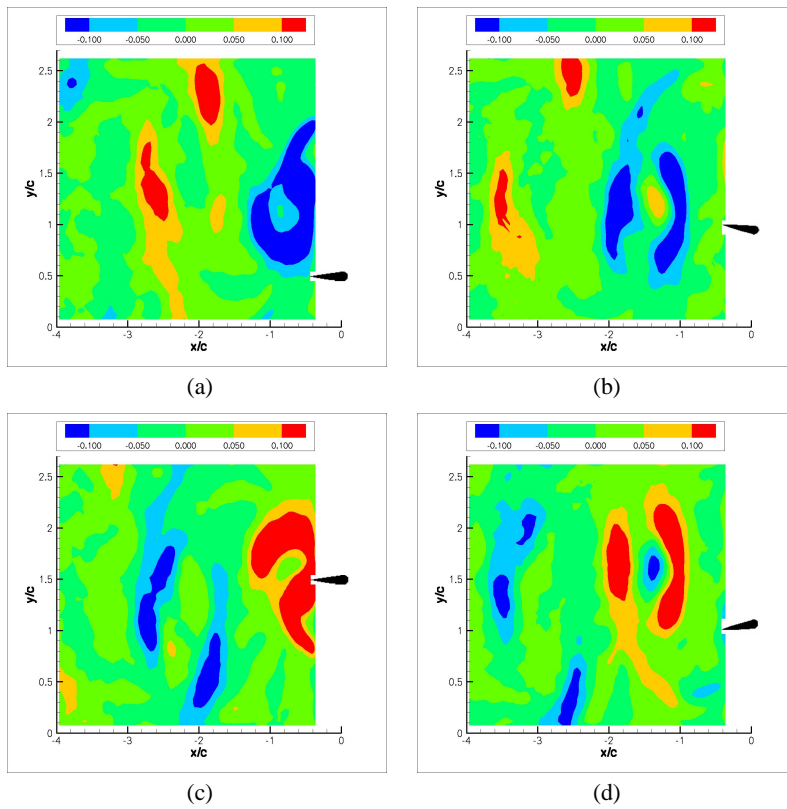


Figure 4: Contour plot of the out-of-plane vorticity ω_z/ω_θ behind a 3D flapping foil at (a) phase 1, (b) phase 3, (c) phase 5, (d) phase 7; where vorticity is non-dimensionalised by the angular velocity of the pitching oscillation of the flapping foil.